Available online at www.sciencedirect.com

ScienceDirect

Journal of Geodynamics 42 (2006) 95–114

JOURNAL OF GEODYNAMICS

http://www.elsevier.com/locate/jog

Three-dimensional numerical thermal and rheological modelling in the central Fennoscandian Shield

K. Moisio *, P. Kaikkonen

Department of Geophysics, University of Oulu, P.O. Box 3000, FIN-90014 Oulu, Finland

Received 13 September 2005; received in revised form 17 May 2006; accepted 30 May 2006

Abstract

A three-dimensional model for the central Fennoscandian Shield was constructed for analysing the thermal, the rheological and the structural conditions in the lithosphere. The mesh covers a rectangular area in the southern Finland with horizontal dimensions of 500 km × 400 km and a depth extent of 100 km. Structural boundaries are derived from the several deep seismic soundings carried out in the area. Constructed model is first used in the calculation of the thermal and the rheological models and secondly in analysing the stress and the deformational conditions with the obtained rheology. Thermal and structural models are solved with the finite element method. The calculated surface HFD is between 40 and 48 mW m^{-2} in the Proterozoic southern part and below 40 mW m^{-2} in the older and northern Archaean part of the model. The calculated rheological strength shows a layered structure with two individual rheologically weak layers in the crust and strong layer in the upper part of the lower crust. The minimum brittle–ductile transition (BDT) depth is around 10 km in the southern part of the model while in the north and north-eastern parts the BDT depth is around 45–50 km. Comparison with the focal depth data shows that as most of the earthquakes occur no deeper than the depth of 10 km are they located in the brittle regime. Resulting stress conditions and possible regions of deformation after the model is subjected to pressure of 50 MPa reveals that the stress field is quite uniformly distributed in different crustal layers and that the elastic parameters control more the state of the stress than the applied rheological structure. In the upper crust, the stress intensity has values between 42 and 45 MPa whereas in the middle crust the values are around 50 MPa. Comparison of the 3-D model with earlier 2-D models shows that some differences in the results are to be expected.

Keywords: Fennoscandian Shield; Lithosphere; 3-D finite-element modelling; Thermal analysis; Rheological strength

1. Introduction

The Fennoscandian Shield is an old and stable continental lithosphere. It is characterized by a few distinct features, i.e., a very thick crust where Moho depth as deep as 65 km (Luosto, 1997) is found, a tectonic quiescence with relatively few and small magnitude of the earthquakes (Ahjos and Uski, 1992) and further a rather cold geothermic structure (e.g., Čermák et al., 1993; Kukkonen, 1998). These features have been revealed by a numerous geophysical investigations that have been conducted during last few decades. The seismic structure is perhaps best known from several deep seismic sounding (DSS) profiles like BALTIC, SVEKA, FENNIA and BABEL (Grad and Luosto, 1987; Luosto et al., 1990; BABEL Working Group, 1993; FENNIA Working Group, 1998). Also heat flow in the surface and vertical

* Corresponding author. Fax: +358 8 5531414.
E-mail addresses: kari.moisio@oulu.fi (K. Moisio), pertti.kaikkonen@oulu.fi (P. Kaikkonen).

0264-3707/$ – see front matter © 2006 Elsevier Ltd. All rights reserved.
doi:10.1016/j.jog.2006.05.001

thermal structure have been investigated and modelled quite intensively (e.g., Puranen et al., 1968; Kukkonen, 1993; Jokinen and Kukkonen, 2000). Electromagnetic measurements have been performed in several projects revealing the electrical structure in crustal and lithospheric scale (e.g., Ádám et al., 1982; Kaikkonen et al., 1983; Korja and Hjelt, 1993; Korja, 1997). All relevant geophysical information of the lithospheric structure is required and facilitates the rheological and structural models, which furthermore can give estimates of the possible deformational conditions in the lithosphere.

Cloetingh and Banda (1992), Dragoni et al. (1993), Kukkonen and Peltonen (1999), Kaikkonen et al. (2000), Pasquale et al. (2001) and Kukkonen et al. (2003) have done one-dimensional (1-D) rheological studies for the Fennoscandian Shield. Moisio et al. (2000) and Moisio and Kaikkonen (2001, 2004) have furthermore used calculated two-dimensional (2-D) rheological structures to define the deformational limits in 2-D finite-element models where the consequences of the rheology were studied. As the optimum boundary condition direction has been restricted in the 2-D cases we have expanded our model to three dimensions. In this paper, we have constructed a three dimensional (3-D) model first time for the central Fennoscandian Shield based on the known deep structure. This model is first used in the calculation of the thermal and the rheological models and secondly in analysing the stress and the deformational conditions with the obtained rheology.

2. Geology and geophysics

The Fennoscandian Shield being a part of an old continental lithosphere was formed between the middle Archaean and middle Proterozoic times. The central part of the Shield, where our model area is located (Figs. 1 and 2) was mainly formed during the Svecofennian orogeny (~1.9–1.75 Ga), which created the anomalously thick crust. This area is characterized by granitoid intrusions emplaced during the orogeny like the large Central Finland Granitoid Complex located in the middle of the model area. Towards the north and northeast geological age increases and older rocks generated during the Archaean orogenies (~2.8–2.6 Ga) exist, which are mainly granites and greenstones. Last major tectonic episodes (~1.7–1.55 Ga) produced anorogenic rapakivi granites, anorthosites and mafic dykes to the southern Finland and slightly later (~1.5–1.2 Ga) some sandstones in the SW Finland. For detailed description of the geology of the Fennoscandian Shield, see e.g., Gaal and Gorbatschev (1987) and Lehtinen et al. (2005).

Seismic research for determining the deep structure of the lithosphere has been widely applied in the central Fennoscandian Shield. First major refraction seismic project was the DSS profile SVEKA (Grad and Luosto, 1987) measured as early as in 1981 (Fig. 1). It was performed as an international co-operation similarly as the later BALTIC profile (e.g., Luosto et al., 1990), which was measured in following summer of 1982. The SVEKA profile was furthermore continued in 1991 and together with the original profile they consist nearly 700 km of seismic soundings crossing the southern and central part of Finland from the Proterozoic to the Archaean domain (e.g., Luosto et al., 1994; Yliniemi et al., 1996). Results from these profiles have revealed a very thick crust, up to 65 km in the central Fennoscandian Shield. Later on deep seismic studies have been performed in profiles such as the FENNIA and the BABEL (Fig. 1) where both refraction and reflection data has been obtained. The FENNIA profile running from south to north is located between the SVEKA and the BALTIC profiles and results from this measurement have shown similar features as in the neighbouring profiles (FENNIA Working Group, 1998). The BABEL project consisted of more than a single profile. It was a large-scale international deep seismic marine reflection experiment with more than 2000 km of profiles carried out in the Baltic Sea and in the Gulf of Bothnia (BABEL Working Group, 1993; Korja and Heikkinen, 1995). These seismic measurements all together have revealed crustal features in very high details. Crustal thickness is well shown in the Moho depth map (Fig. 1) where the areas of very deep Moho boundary are clearly visible. A large seismic reflection experiment (FIRE—Finnish Reflection Experiment) has been performed recently covering Finland from south to north with over 2100 km of measured profiles (Kukkonen et al., 2002). This experiment will provide new valuable data in near future also for analysis of the rheological structure.

Seismic tomography research for the central Fennoscandian Shield, i.e., the SVEKALAPKO project was accomplished in the late 1990s with 143 seismic stations deployed in an array of 1000 km × 900 km. That study focused on the deep structure of the lithosphere–asthenosphere system up to the depth of 400 km and the latest results suggest that no seismic asthenosphere could be definitively found in the central Fennoscandian Shield (Sandoval et al., 2004). Earlier studies (Calcagnile, 1982; Babuska et al., 1988) have estimated the thickness of the lithosphere to be between 180 and 190 km. Thermal studies in which geotherms are calibrated with xenolith data estimate the thermal and rheological lithosphere to be at least 230–250 km thick (Kukkonen et al., 2003).

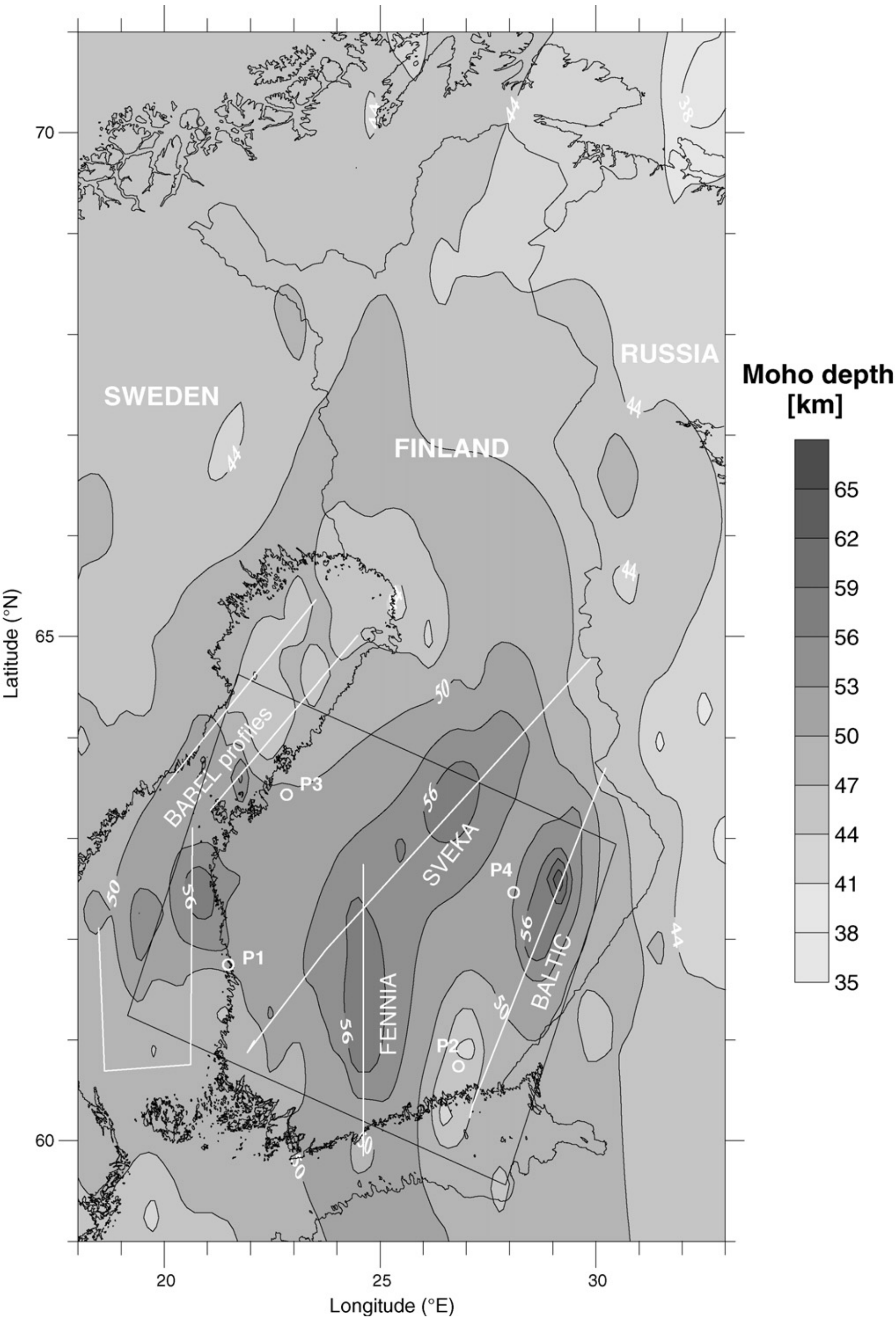

Fig. 1. The relevant DSS profiles and the model area outlined above a Moho depth map for the central Fennoscandian Shield. Points P1, P2, P3 and P4 refer to locations used in Fig. 9.

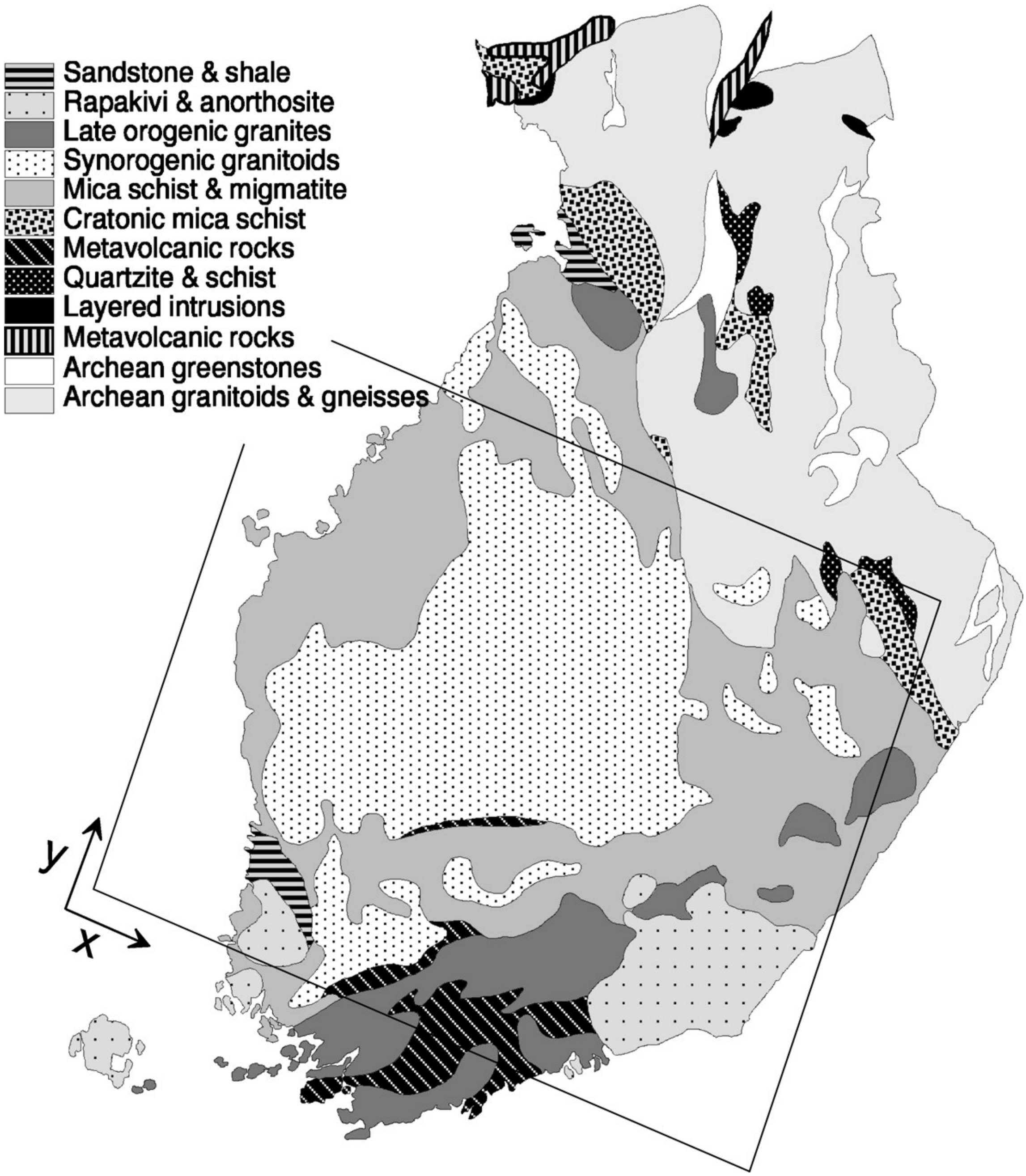

Fig. 2. Simplified geological map of the central Fennoscandian Shield with model area outlined. Origin and the direction of the *x*- and *y*-coordinate axis for the model are also shown. *z*-Axis is vertical.

Geothermal research in the central Fennoscandian Shield has been quite intensive and the first report of the measured heat flow densities (HFD) has been published in the late 1960s (Puranen et al., 1968). There are approximately 30 HFD measurement sites in the area relevant to our study and some 50 sites overall in the Finland. These results are published by Järvimäki and Puranen (1979) and Kukkonen (1988, 1989a,b, 1993). The HFD map (Fig. 3) shows that generally values of the heat flow are quite low, below 40 mW m^{-2}, but also some anomalously high values are observed. Generally lower values are found in the older Archaean areas. The arithmetic mean for all measured HFD values in Finland is 37 mW m^{-2}. Geothermal modelling has also been widely applied for investigating the deep thermal structure in the

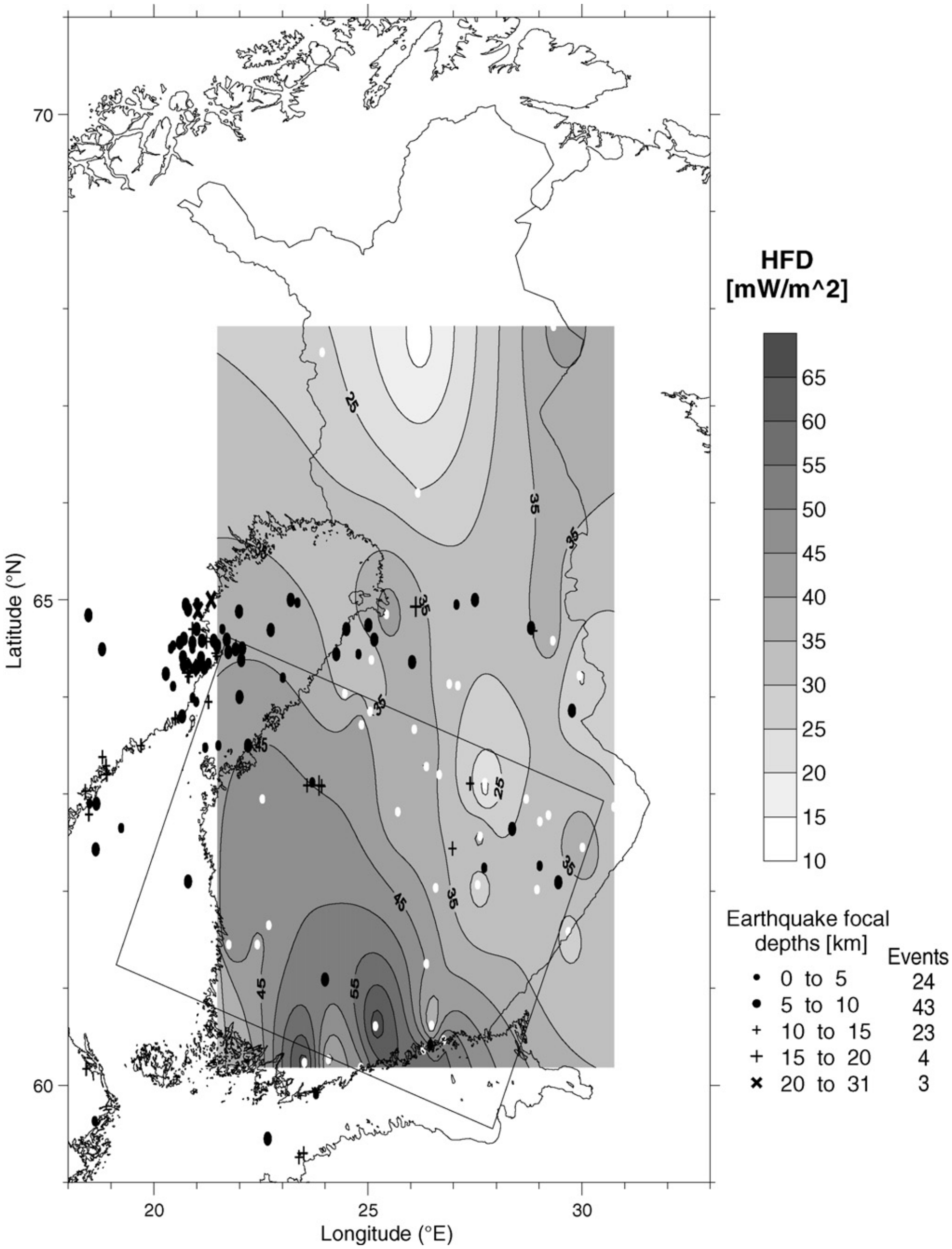

Fig. 3. Heat flow density map for the central Fennoscandian Shield together with the earthquake epicenters and their focal depths for the area of 18–32°E and 59–65°N. White dots are the places of the HFD measurements sites.

Fennoscandian Shield (e.g., Pasquale et al., 1991; Čermák et al., 1993; Kukkonen, 1995, 1998; Kukkonen and Jõeleht, 1996). These modellings are usually connected to vicinity of the DSS profiles as seismic models provide relevant data, i.e., indications of the petrology and the thermal properties of the deep structure. In the central Fennoscandian Shield detailed studies for evaluating crustal heat production have shown that values of heat production can have a quite large variability between different lithological and tectonic units and in general these values are decreasing with increasing geological age (Kukkonen, 1989a, 1998; Jõeleht and Kukkonen, 1998; Kukkonen and Lahtinen, 2001).

Earthquake activity in Finland is generally quite low and the magnitudes of the earthquakes are relatively small, usually a local magnitude M_L around two (Ahjos and Uski, 1992). Epicenters and their focal depths in Fig. 3 show that the highest earthquake activity is found in the western part of the area in question. In southern Finland the number of earthquakes is quite small, therefore earthquake data for our model area can only be considered indicative. Focal depths of the earthquake data show that most of the events occur at a depth smaller than 15 km (Fig. 3; see also Fig. 9d). Fault plane solutions for the Finnish earthquakes are presented in Uski et al. (2003). The number of these solutions is quite low due to a sparse coverage of seismic stations and the small magnitudes of Finnish earthquakes, but lately improvements have been made in upgrading the station instruments and coverage and also in the fault plane solution techniques (Uski et al., 2003). These older solutions show dominantly strike-slip with some dip-slip movement along nearly vertical planes with maximum horizontal compression approximately in NW–SE direction indicating that major component in generating the stress field in Finland is the ridge-push from the North Atlantic. The latest fault plane solutions (Uski et al., 2003) show that also thrust and normal fault mechanisms are found from the Finnish earthquakes. Data from the world stress map project (Reinecker et al., 2004) which are based on borehole measurements in the uppermost crust indicate that a primary mechanism is thrust faulting. Together with geodetic observations (Chen, 1991; Kakkuri, 1997) these also imply that the stress field in Finland is mainly dominated by the NW–SE oriented compression, but some differences due to the postglacial rebound and other local factors are found. In situ stress data for Finland is available in few sites. These measurements indicate similar stress conditions as in previously mentioned data. Values of over 40 MPa for the maximum horizontal stress have been measured in boreholes (Klasson and Lejon, 1990).

Analysis of the rheological structure and 2-D structural finite element models (Kaikkonen et al., 2000; Moisio et al., 2000; Moisio and Kaikkonen, 2001, 2004) have shown that central Fennoscandian Shield can be considered rheologically rather strong although variations on the results can be generated with different material and thermal conditions. State of stress and deformation in the lithosphere based on these models mainly suggest low level of ductile deformation and concentration of the stresses to the lower crust and the upper mantle.

3. Background theory

Rheology defines how material behaves when it is subjected to deforming forces. Rate and type of deformation is controlled by the intrinsic properties of the material, e.g., mass, rigidity, viscosity, grain size, etc. and also by the external conditions, e.g., temperature, pressure, strain-rate, etc. (Carter and Tsenn, 1987). In lithosphere two principal modes of deformation are recognized, brittle and ductile mechanisms. For deformation to occur differential stress, defined as the difference between the largest σ_1 and the smallest σ_3 principal stress, must exceed materials, i.e., rocks yield strength. For the brittle deformation this limit is often expressed with the Byerlee's law (see e.g., Ranalli, 1995)

$$\sigma_1 - \sigma_3 = \alpha\rho g z(1 - \lambda), \tag{1}$$

where ρ is the density, g the gravitational acceleration, z the depth, λ the hydrostatic pore fluid factor (ratio of pore fluid pressure to overburden pressure) and α is a parameter depending on the fault type. We have used following values: $\alpha = 3$, which is a result of a friction coefficient value of 0.75 for thrust (compressional) faulting and $\lambda = 0.35$ as the upper part of the crust is often assumed to have some water occupying the pore space. For the middle and upper crust, we have assumed wet and for the lower crust dry conditions for the brittle mechanism. With value $\alpha = 3$ in the compressional regime strength has maximum values, if assuming normal/strike-slip faulting strength values are lower, i.e., $\alpha = 0.75/1.2$.

For the ductile deformation yield strength is expressed with the ductile flow law, i.e., the creep law, from which two different types of mechanisms are used, the power law (Eq. (2)) and the Dorn law (Eq. (3)) relations (Goetze and Evans, 1979; Tsenn and Carter, 1987; Ranalli, 1995). The flow law gives the stress difference necessary to achieve a given strain rate

$$\sigma_1 - \sigma_3 = \left(\frac{\dot{\varepsilon}}{A_\mathrm{p}}\right)^{1/n} \exp\left(\frac{E_\mathrm{p}}{nRT}\right), \tag{2}$$

$$\sigma_1 - \sigma_3 = \sigma_\mathrm{D}\left[1 - \left(-\frac{RT}{E_\mathrm{D}} \ln\left(\frac{\dot{\varepsilon}}{A_\mathrm{D}}\right)\right)^{1/2}\right] \tag{3}$$

Table 1
Material parameters used in geothermal, rheological and structural modelling (from Carter and Tsenn, 1987; Carmichael, 1989; Wilks and Carter, 1990; Ranalli, 1995; Kukkonen, 1998)

Layers	Petrology	Power law exponent n	Activation energy E_p (kJ mol^{-1})	Initial constant A_p (MPa^{-n} s^{-1})	Thermal conductivity k (W m^{-1} K^{-1})	Heat production A (μW m^{-3})	Density ρ (kg m^{-3})	Young's Modulus E (GPa)	Poisson's ratio μ
Upper crust	Granite (wet)	1.9	140	2.0E−04	3.0	1.6–0.9	2700	60	0.23
Middle crust	Diorite (wet)	2.4	212	3.2E−02	3.0	0.6–0.3	2800	70	0.25
Lower crust	Mafic granulite (dry)	4.2	445	1.4E+04	3.0	0.1–0.05	2900	80	0.27
Mantle	Olivine (dry)	3.0	510	7.0E+04	4.2	0.02–0.002	3100–3300	70	0.25
	Flow parameters for the Dorn law								
	Petrology	Activation energy E_D (kJ mol^{-1})	Initial constant A_D (s^{-1})	Dorn law stress σ_D (GPa)					
Mantle	Olivine	535	5.7E+11	8.5	4.2	0.02–0.002	3100–3300		

where A_p, n and E_p are empirically determined material parameters for the power-law (see Table 1), T the temperature, $R = 8.314\,\mathrm{J\,mol^{-1}\,K^{-1}}$ (universal gas constant) and $\dot{\varepsilon}$ is the strain rate. We have used a uniform strain rate of $\dot{\varepsilon} = 1 \times 10^{-15}\,\mathrm{s^{-1}}$. At higher differential stresses (>200 MPa) for olivine mineralogy the Dorn law is used instead of the power law (e.g., Tsenn and Carter, 1987). In the ductile regime also assumption of whether rock is dry or wet is made upon creep parameters. Hydrous environments can possibly occur in the crust and the mechanism of hydrolytic weakening reduces the ductile strength considerably. We have assumed the upper and middle crustal conditions to be wet and for the lower crust dry for the ductile mechanism.

In thermal modelling, we have taken into account the temperature dependence of the thermal conductivity following the relationship

$$k(T) = k_{\mathrm{ref}}\left[\left(\frac{1}{1+bT}\right) + c(T + 273.15\,\mathrm{K})^3\right] \tag{4}$$

where T is the temperature (°C), k_{ref} the thermal conductivity at the room temperature ($\mathrm{W\,m^{-1}\,K^{-1}}$) and b and c are empirical constants ($b = 0.0015\,\mathrm{K^{-1}}$, $c = 1 \times 10^{-10}\,\mathrm{W\,m^{-1}\,K^{-4}}$).

4. Numerical modelling

4.1. Model construction

Our mesh covers a rectangular area in the southern Finland with horizontal dimensions of 500 km × 400 km (Fig. 1) and a depth extent of 100 km containing approximately 125,000 nodes and 57,000 elements. Most of the elements are octagonal in shape having either 8 or 20 nodes depending on the location while few are tetrahedral. Element sizes in the vertical direction are generally around 3–4 km and they have been kept as small as possible especially in vicinity of the Moho boundary. Horizontal sizes are higher and they have also more variation. The depth of the model has been limited to 100 km due to computational resources although the lithosphere–asthenosphere boundary would be 'natural' choice. However, this limitation allows better resolution in the upper part of the model and likely most interesting rheological features are found in the upper 100 km of the lithosphere. Our mesh is oriented so that its longest axis is approximately in the same direction as the assumed maximum horizontal stress, i.e., NW–SE. This way the applied boundary conditions are oriented optimally in comparison to the orientation of the in situ stress conditions as discussed earlier. Horizontal boundaries of the mesh are derived from the seismic models while vertical boundaries are not actual seismic borders, they are merely used to divide the volume to smaller units where different material conditions exist. Horizontal boundaries divide the crust into the upper, the middle and the lower crust. This division is approximately based on the P-wave velocity isolines of 6.3–6.4 $\mathrm{km\,s^{-1}}$ for the boundary between the upper and the middle crust, 6.9 $\mathrm{km\,s^{-1}}$ for the middle and the lower crust and the Moho boundary for division between the crust and the mantle. We have tried to keep the model structurally as simple as possible and therefore the finest details found in the seismic velocity sections are excluded.

4.2. Material parameters

Material parameters are chosen so that they are representative of typical rock types occurring in the research area. Material parameter variation has been kept to a minimum in horizontal directions. Elastic material parameters, i.e., Young's Modulus and Poisson's ratio (Table 1) are taken from Carmichael (1989) for typical rock types occurring in the central Fennoscandian Shield. Also the ratio of P- and S-wave velocities along different seismic profiles were used to confine the Poisson's ratio. Values of densities (Table 1) are taken from the velocity models of different seismic profiles and from the gravity model of Kozlovskaya and Yliniemi (1999) for the SVEKA profile. A simplification is made, as densities are kept constant in each horizontal layer, i.e., in the upper crust 2700 $\mathrm{kg\,m^{-3}}$, in the middle crust 2800 $\mathrm{kg\,m^{-3}}$ and in the lower crust 2900 $\mathrm{kg\,m^{-3}}$. In the mantle densities vary between 3100 and 3300 $\mathrm{kg\,m^{-3}}$. Thermal conductivity follows the temperature dependence given in Eq. (4) with different starting values in the crust and in the mantle (Table 1). Values of the heat production vary in the upper crust between 1.6 and 0.9 $\mu\mathrm{W\,m^{-3}}$, in the middle crust from 0.6 to 0.3 $\mu\mathrm{W\,m^{-3}}$ and in the lower crust between 0.1 and 0.05 $\mu\mathrm{W\,m^{-3}}$. In the mantle values ranging from 0.02 to 0.002 $\mu\mathrm{W\,m^{-3}}$ are used. The heat production is kept constant inside the individual volumes.

Rheological parameters (Table 1) for the yield strength calculations are taken from Carter and Tsenn (1987), Wilks and Carter (1990), Ranalli (1995) and Fernàndez and Ranalli (1997). We have adopted a general petrological classification for the crust and the mantle based on the densities and seismic velocities assuming felsic composition for the upper crust, intermediate for the middle crust, mafic for the lower crust and ultramafic for the mantle. We have approximated these compositions with creep parameters (Table 1) of wet granite and diorite in the upper and the middle crust, respectively, mafic granulite for the lower crust and olivine for the mantle.

4.3. Boundary conditions

Rheological modelling requires knowledge of the thermal structure. The 3-D conductive steady-state model is solved using the finite-element method. The model is subjected to thermal boundary conditions of constant temperature of 5 °C on the surface of the earth and temperature varying between 695 and 730 °C on the base of the model, i.e., depth of 100 km. Choice of these boundary values is based on the results of the earlier thermal models in the SVEKA (Kukkonen, 1998) and the FENNIA (Moisio and Kaikkonen, 2004) profiles. Temperature in these models at the depth of 100 km varied approximately between 660–710 and 690–710 °C, respectively. This horizontal transition in temperature corresponds to a change in the depth of the thermal lithosphere, which is understood to increase gradually towards the Archaean domain (see e.g., Kukkonen, 1998).

Obtained temperature values are used in the calculation of the rheological strength. Strength values are subsequently used as nonlinear material parameters in the structural finite-element model which has the same geometry and element distribution as the thermal one. This structural model is subjected to compressional boundary condition in order to simulate the tectonic stress conditions in the area. Pressure of 50 MPa is applied to the NW vertical facet of the model in the direction of the x-axis, which is the longest horizontal axis while the SE vertical facet is stationary simulating a rigid tectonic plate. The boundary condition of 50 MPa value is chosen by comparing trial and error modelling results with measured stress field values (Saari, 1992). With this value our modelling leads to reasonable and in some sense ‘realistic’ stress field intensities as is nowdays understood about lithospheric stress conditions. These results are however very difficult to verify with measured values as the number of in situ stress measurements are low. The bottom of the model is not allowed to move in the vertical direction. In the y-direction model has no restrictions except for the two nodes, which are not allowed to move in the y-direction. These nodes are located side by side approximately in the centre of the base of the NW facet. This is a computational restriction as it prevents rigid body motion. These two nodes had minimum values in the displacement of the y-coordinate in a model case, which had no restrictions in the y-direction. The structural model is solved with the finite-element method assuming a steady-state condition. Also the gravity is neglected, i.e., only the deviatoric state of the stress is analysed. All finite-element calculations were done with the software package ANSYS^{TM}.

4.4. Uncertainties in thermal models

Temperature has a major influence on rheological models as it controls the ductile flow laws. However, uncertainties related to temperature estimations in the crust and the mantle are quite large, as many different sources of error exist. There are errors related to measurement of the borehole temperatures, i.e., groundwater flow, erosion, paleoclimatic effects, etc. (see e.g., Kukkonen, 1989a, 1995; Kukkonen and Jõeleht, 2003) bias the results. Thus derived surface HFD values can be inaccurate, for example variation in the surface HFD with an amount of $\pm 10\,\mathrm{mW\,m^{-2}}$ changes the temperature at the depth of 50 km approximately ±100 °C. Errors related to calculation of the geotherms are largely connected to determining thermal conductivity and heat production values of the crust and the mantle (Jokinen and Kukkonen, 1999; Kukkonen et al., 1999). Importance of these two parameters is widely known and estimation of proper values is a fundamental problem in thermal modelling as these are mainly indirectly estimated for the lithosphere. Thermal conductivity varies only little in typical lithospheric rock types and is usually between values of 2 and $4\,\mathrm{W\,m^{-1}\,K^{-1}}$, but conductivity is also dependent on the temperature. Values of heat production can vary between a much larger range. Between the low values of the depleted mantle and high ones of the upper crust there can be a difference of three decades. Heat production values measured from outcrops and till samples provide estimates for values of the uppermost crust. Difficulties arise when heat production values for rest of the lithosphere are determined. Relationships between the heat flow–heat production, the seismic P-wave velocity–heat production and the lithological models of the lithosphere based on the DSS data can be used to overcome this problem.

Variations in thermal conductivity and heat production can result in similar amount of temperature change at the 50 km depth as the HFD variation of $\pm 10\,\mathrm{mW\,m^{-2}}$. However, numerous efforts have been made to improve the temperature models. For example, random modelling has been applied (Jokinen and Kukkonen, 1999) where thermal parameters vary randomly between specified ranges. As a result deviations in the temperature and the surface HFD are determined for different parameter uncertainties. Also xenolith-controlled geotherms have been calculated (Jokinen and Kukkonen, 2000; Kukkonen and Peltonen, 1999) where temperature in the mantle is constrained from xenolith derived data. Uncertainties in thermal modelling were also discussed in Moisio and Kaikkonen (2004) where thermal models generated with different boundary conditions and thermal parameter values were compared.

4.5. Uncertainties in rheological models

Results of rheological modelling are subjected to many uncertainties like the earlier discussed temperature. Different thermal models and their effect to rheological calculations were analysed in more detail by Moisio and Kaikkonen (2004). Fernàndez and Ranalli (1997) have divided the uncertainties related to rheological calculations into two groups; operational and methodological. Operational errors include inaccurate estimation of lithospheric structure and composition, errors in temperature, improper material and rheological parameters, pore fluid pressure and friction coefficient, etc. Also existence of hydrous environment together with assumption of tectonic setting, i.e., faulting type has to be considered. One significant error is related to rheological parameters themselves. Fernàndez and Ranalli (1997) have compiled widely used parameters for different lithospheric layers and they found a large variation among them. Selecting a proper value for the rheological parameter is a difficult task as significant differences in the rheological strength can be introduced. Methodological errors include for example inaccurate rheological flow laws both in the brittle and the ductile regime and also assumption of the uniform strain and constant strain rate. It is advisory to keep in mind that the rheological flow laws are derived from experimental data, which are furthermore extrapolated to lithospheric conditions. The brittle failure criteria defined by the Byerlee's law has been derived from results that have been confirmed only to a depth of few kilometres and therefore application of it to much larger depths results in strengths that are most likely somewhat unrealistic. Different brittle mechanisms are also very likely to occur in the deeper parts of the lithosphere as pressure increases (Ord and Hobbs, 1989; Shimada, 1993). Also ductile flow mechanism can differ from the commonly used at least for some compositions, e.g., peridotite (e.g., Drury et al., 1991). Strain rate and its effect to rheological strength was analysed in more detail in Kaikkonen et al. (2000) and also in Moisio and Kaikkonen (2001).

With all these uncertainties and assumptions made one should always carefully analyse and consider results of the rheological calculations. However, some assumptions of the rheological conditions in the lithosphere can be made from the results if error limits are recognized.

5. Results and discussion

5.1. Thermal model

Calculated thermal structure for the 3-D model is shown in Fig. 4. The solid black lines in the slice planes show the different crustal layers, i.e., the upper, the middle and the lower crust and the mantle so that the lowest solid line is the Moho. The horizontal slice plane above the vertical ones shows the temperature distribution at the depth of 50 km. These temperature values at the depth of 50 km are approximately between 490 and 420 °C. Temperature is generally higher in the southern part of the model, i.e., temperature decreases as the *y*-coordinate increases towards the north and the older Archaean area. In the FENNIA profile (Moisio and Kaikkonen, 2004) temperature varied at the same depth from 470 to 440 °C and in the SVEKA models from 510 to 470 °C (Moisio and Kaikkonen, 2001) and from 500 to 350 °C (Kukkonen, 1998). There is a small difference between temperature values in the SVEKA models (Moisio and Kaikkonen, 2001). The SVEKA profile was calculated with slightly different procedure, as there was no dependence between thermal conductivity and temperature and so the results are not fully comparable particularly for the deeper parts. This comparison however shows that these results are in concordance with previous thermal models done in the region as intended although some discrepancy is found, also with more recent xenolith-controlled geotherms (Kukkonen and Peltonen, 1999). A comparison between the calculated HFD values (Fig. 5) with the measured ones (Fig. 3) shows the most significant differences between these data sets. Large HFD gradients seen in measured values

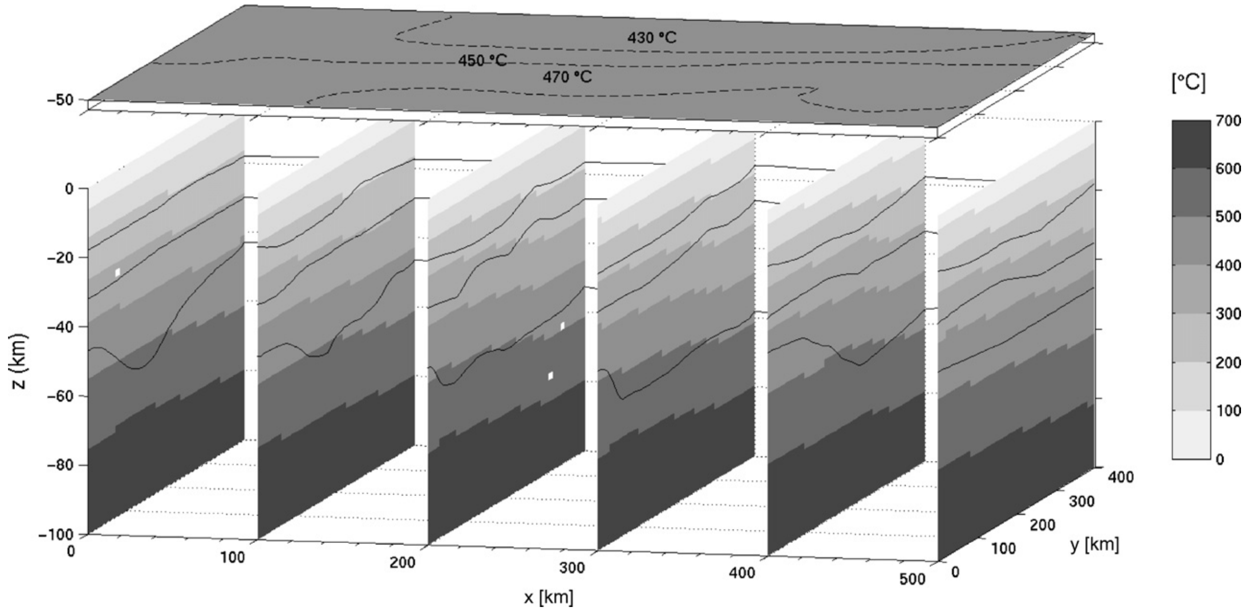

Fig. 4. Calculated temperature in the model shown for vertical slice planes in positions $x = 0$, 100, 200, 300, 400 and 500 km. Horizontal slice plane above the vertical ones shows the temperature at the depth of 50 km with contour interval 20 °C. For the orientation of the x-and y-axes see Fig. 2. Note that in all following figures horizontal and vertical scales are not equal.

are absent and behaviour of the calculated HFD is much smoother than the observed field. This difference implies that some of the measured HFD values are probably strongly affected by local thermal conditions and/or by errors connected to the calculation of the geotherms and the HFD determination. On the other hand, our thermal model is coarse as it has no horizontal variation in the thermal properties of the lithosphere. Although crustal heat production has horizontal variation it is possible that much larger differences in smaller units could result in more or less similar surface HFD as the measured one. Generally the calculated surface HFD is between 40 and 48 mW m^{-2} in the Proterozoic southern part and below 40 mW m^{-2} in the older Archaean and northern part of the model. At the depth of 50 km the

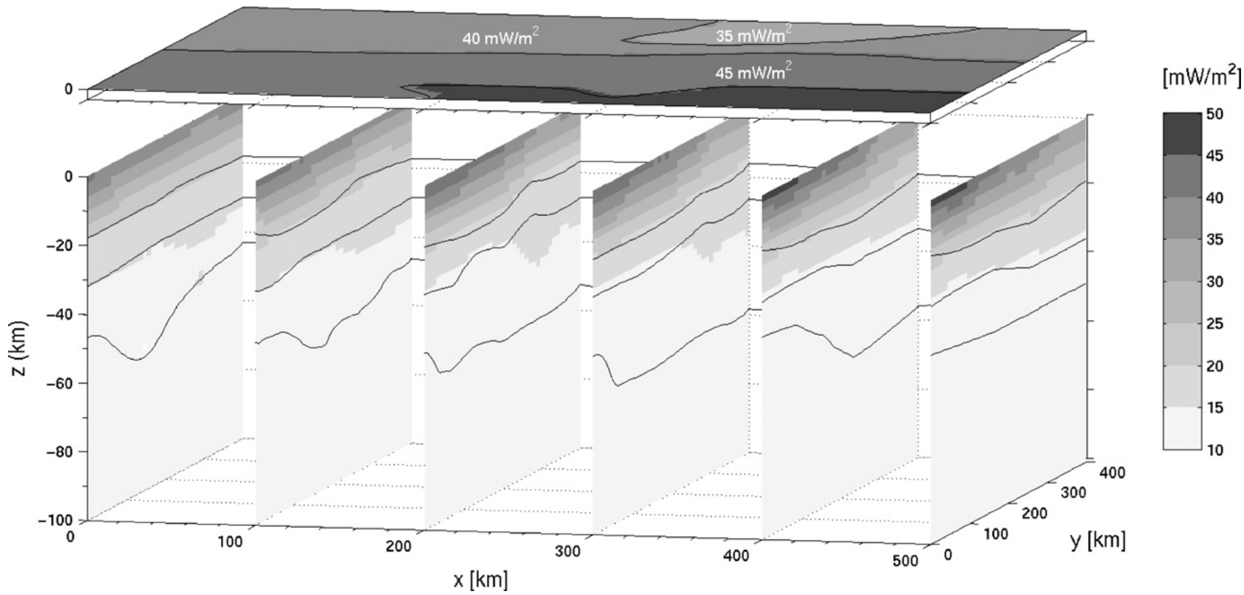

Fig. 5. Calculated heat flow density (HFD) in the model shown for vertical slice planes in positions $x = 0$, 100, 200, 300, 400 and 500 km. Horizontal slice plane shows the surface heat flow density with contour interval 5 mW m^{-2}.

HFD has values around 12 and 14 mW m^{-2} and even slightly lower deeper in the mantle. In the 2-D model of the FENNIA profile (Moisio and Kaikkonen, 2004) the surface HFD values varied between 38 and 46 mW m^{-2} and at the depth of 50 km quite close to 13 mW m^{-2} whereas in the SVEKA profile the surface HFD values were between 34 and 42 mW m^{-2} (Moisio and Kaikkonen, 2001).

5.2. Rheological model

The calculated rheological structure in the 3-D model has similar features as seen in the earlier 2-D rheological models (Moisio and Kaikkonen, 2001, 2004). For the deformation of the crust the most significant regions are those where the strength has diminished to values low enough for tectonic stresses to exceed them. Estimations of in situ stresses are mainly based on stress measurements in boreholes, which are limited to a depth of a few kilometres at most, and conditions deep in the crust can only be indirectly estimated. In Finland these measurements have given maximum values over 40 MPa for the horizontal stress (Klasson and Lejon, 1990). It is estimated that critical stresses in the crust are unlikely to exceed values of 200 MPa (Lamontagne and Ranalli, 1996; Ranalli, 2000). Cross-section of the rheological strength (Fig. 6) shows a layered structure in the crust with two individual rheologically weak layers in the granitic upper and the dioritic middle crust with strength values below 200 MPa. The depths of these layers are approximately between 11–17 and 23–32 km, respectively, however they are quite thin, only about 3–4 km in maximum. These layers are more continuous in the southern area of the model while parts of them disappear in the west and most in the north. Above these layers is also located the transition zone, i.e., the region of the maximum strength, where deformation mechanism changes from brittle to ductile (brittle–ductile transition-BDT). Depth of the uppermost transition zone varies quite a lot depending whether weak zones in the crust are present or not. The minimum BDT depth is around 10 km in the southern part of the model while in the north and north-eastern parts where no weak zones are present the rheological strength increases following the linear relation (Eq. (1)) down to the lower crust and thus the BDT depth is as deep as 45–50 km. This uppermost BDT depth is very often described as the lower limit of earthquake occurrence. This limit can also be defined as a depth where the frictional behaviour changes and for granitic composition this transitional temperature is approximately 350 °C (Scholz, 1990; Blanpied et al., 1991). This temperature in our thermal model lies between depths of 29 and 41 km so that the lowest values are in the southern and the largest ones in the northern part. These values are in the same range as in the 2-D FENNIA profile, where the depth of the 350 °C isotherm was between 34 and 37 km (Moisio and Kaikkonen, 2004).

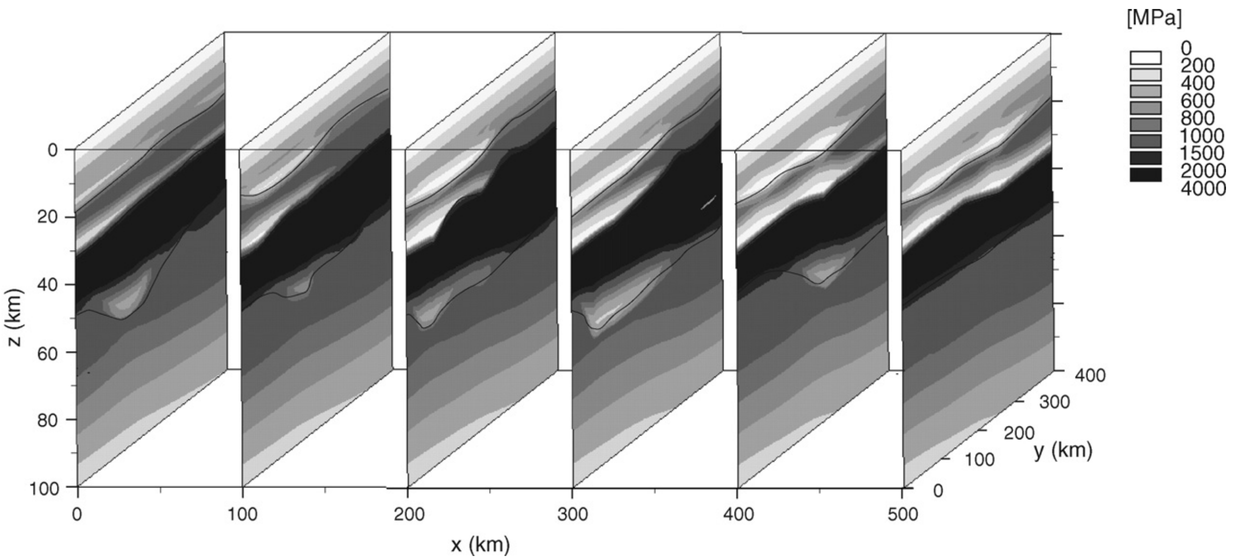

Fig. 6. The rheological strength for compressional conditions (thrust faulting) shown with vertical slice planes in positions $x = 0$, 100, 200, 300, 400 and 500 km. Lithology is wet granite and diorite in the upper and the middle crust, respectively, dry mafic granulite for the lower crust and olivine for the mantle. Note that the contour levels are not uniform.

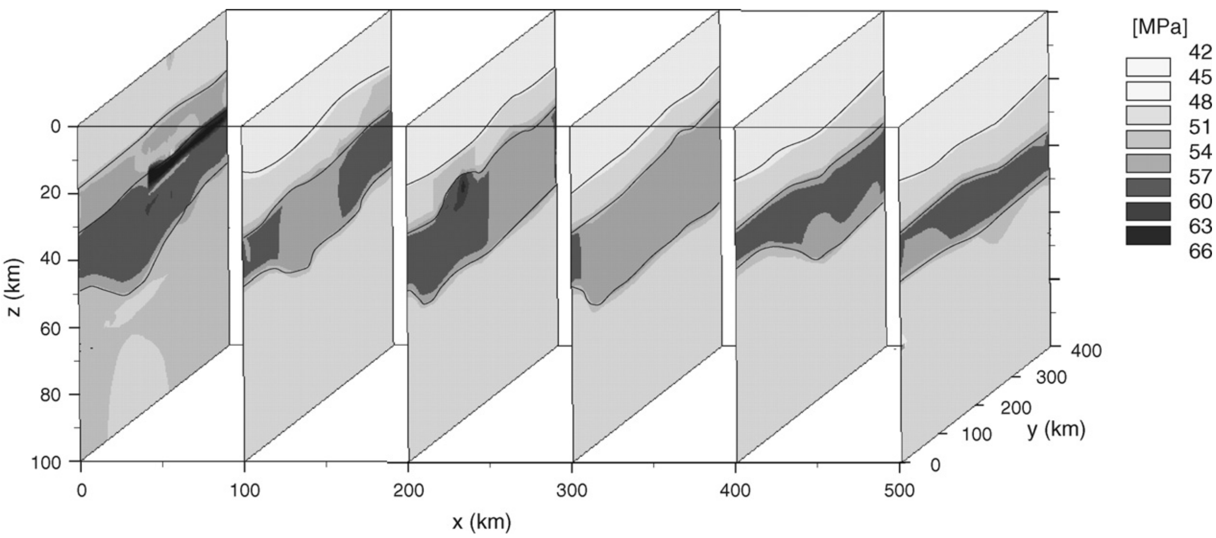

Fig. 7. The stress intensity generated with the compressional boundary condition of 50 MPa applied to the NW vertical facet, i.e., $x = 0$ shown with vertical slice planes in positions $x = 0$, 100, 200, 300, 400 and 500 km. Values above 66 MPa are shown in black.

Earthquake events in southern Finland (18–32°E, 59–65°N) are quite rare, but during the time period of 1965–2004 about 240 events were recorded and from them approximately 100 focal depth estimations have been done (Uski and Pelkonen, 2004). This data shows (Fig. 3) that most of the earthquakes, nearly 70%, occur no deeper than 10 km and they are also quite uniformly spread between depths from 3 to 10 km. Comparison with the rheological structure shows that most of these events are located in the brittle regime. However, the rheological strength in the brittle region of the upper crust gains rather large values with the used parameters. For example, at the depth of 10 km it is required to have critical stresses above 500 MPa for the failure of rock which is in contradiction with the observed earthquake focal depths and assumed maximum intraplate stresses. This can be explained with higher pore fluid pressures (λ in Eq. (1)) or lower friction coefficient value. These parameters alone or together can maintain more reasonable critical stresses (see e.g., Ranalli, 2000). Also a different type of deformation mechanism, i.e., a high-pressure type fracture where the strength does not grow linearly as a function of the depth but instead remains almost constant (Shimada, 1993) would explain the contradiction.

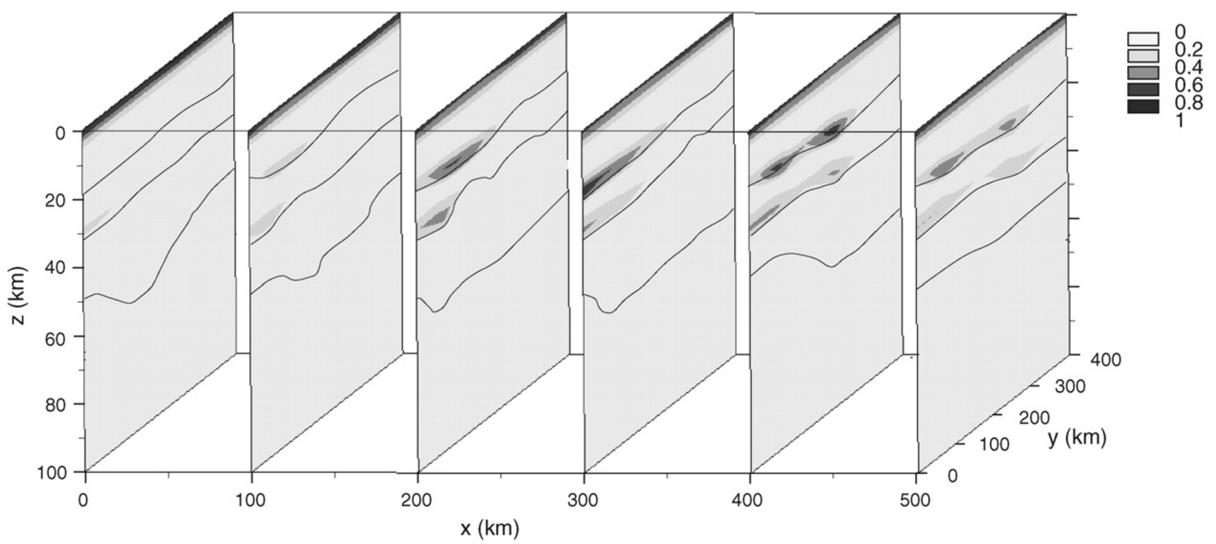

Fig. 8. The stress ratio generated with the compressional boundary condition of 50 MPa shown with vertical slice planes in positions $x = 0$, 100, 200, 300, 400 and 500 km.

Non-existence of the deeper earthquakes can be explained for example with high strength in the middle and the lower crust. This can be a result of dry conditions, e.g., the pore fluid pressure is low or even zero which leads to high strength values. Also the number of fractures in these areas can be low or they remain stable. In general it can be pointed out that as earthquakes are rare below the depths of 15 km stress conditions in these parts of the crust are such that the tectonic stress is not large enough to exceed the true strength.

A rheologically strong layer located in the upper part of the lower crust made of 'strong' mafic granulite continues through the entire model. As stated above this layer is also the BDT zone in some areas of the model. Rheologically weaker regions are also found in the deepest part of the crust, where Moho depth is close to 60 km. However, the rheological strength in these areas does not reach as low values as in the already mentioned weak layers being in minimum only around 400 MPa. In the mantle the olivine controls the rheology and here the strength decreases as the temperature increases following the relations of the creep equation.

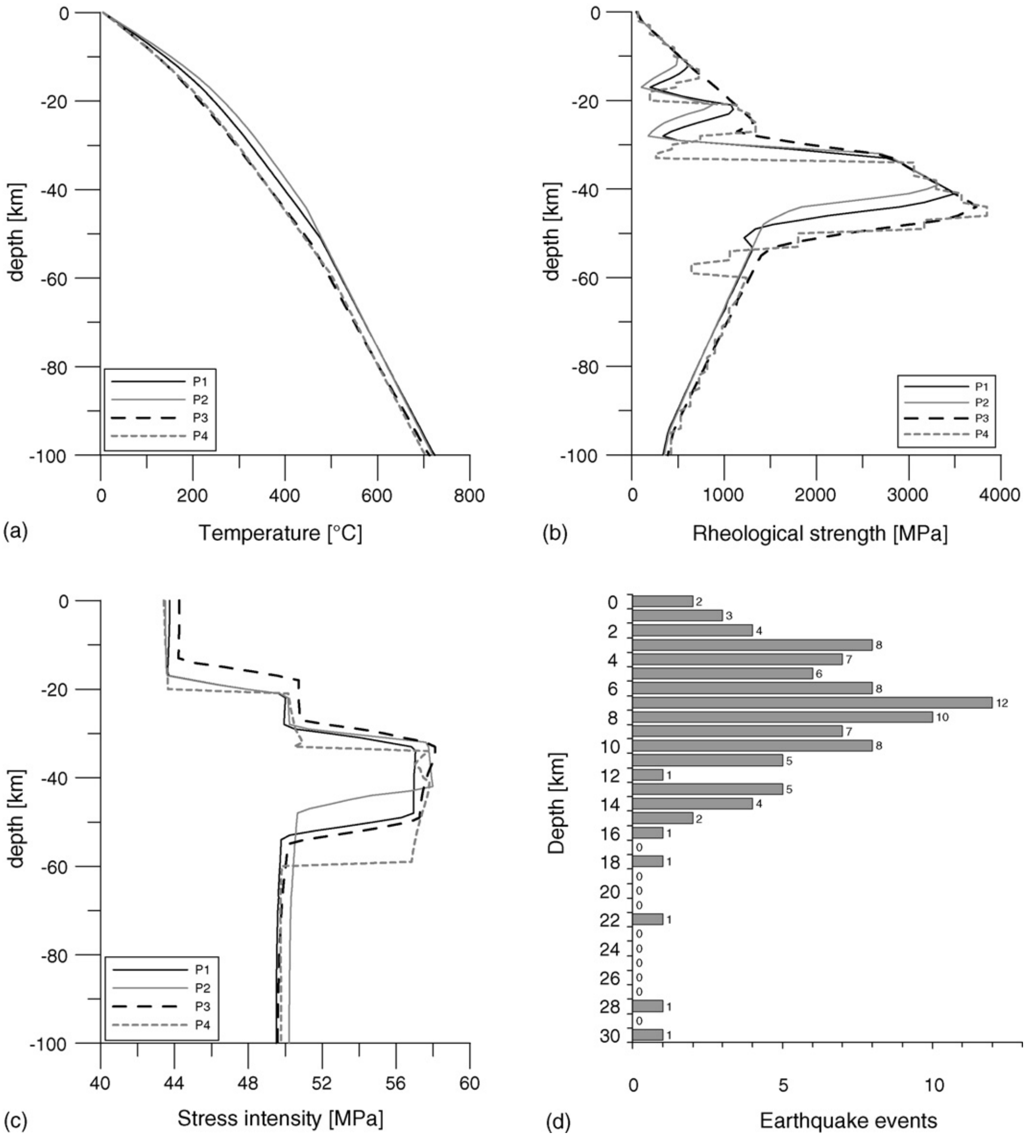

Fig. 9. (a) Temperature, (b) rheological strength, (c) stress intensity as a function of depth in four different locations (P1, P2, P3, P4) of the model area and (d) earthquake focal depth histogram for the central Fennoscandian Shield (18–32E, 59–65N) during 1965–2004. Location of the points (P1, P2, P3, P4) is shown in Fig. 1 and their model coordinates are P1 ($x = 100$, $y = 100$), P2 ($x = 400$, $y = 100$), P3 ($x = 100$, $y = 300$), P4 ($x = 400$, $y = 300$).

Next resulting stress conditions and possible regions of deformation after the model is subjected to pressure boundary condition of 50 MPa are analysed. The orientation of the principal stresses is so that the largest principal stress, showing compressive stress conditions is mainly oriented in the *x*-direction as a result of the applied pressure being parallel to the *x*-axis. The intermediate and the smallest principal stresses show both compressive and tensile conditions in the horizontal *y*-axis and vertical *z*-axis directions, respectively. The magnitude of the largest principal stress is approximately one decade larger than the magnitude of the intermediate or the smallest principal stresses and therefore the state of stress is mostly defined by largest principal stress. The resulting stress condition due the applied boundary condition of 50 MPa is shown in Fig. 7 as the stress intensity. The stress intensity is defined as a largest difference between absolute values of the principal stresses and therefore it has only positive values and no information of compressional or tensional conditions exist unlike in the principal stresses themselves. However, it is a parameter that describes the overall stress conditions as a deviation from the isotropic state and in this particular case as stated above it is very close to the largest principal stress. Large distorted stress values are generated to the NW facet where the pressure of 50 MPa is applied and therefore we have cut off maximum values and the colour scale is adjusted to display the relevant stress interval. In the upper crust the stress intensity has values between 42 and 45 MPa whereas in the middle crust values are around 50 MPa. Also below the Moho stress values have nearly same magnitude as in the middle crust. The highest values around 60 MPa are found in the lower crust. These values seem rather low in comparison with the calculated strength values especially in the upper crust if considered together with the earthquake events. These stress intensities are not capable generating brittle deformation except in the uppermost crust unless the strength values are somehow reduced. The stress field is quite uniformly distributed in different crustal layers and it seems that the elastic parameters control more the state of the stress than the applied rheological structure as practically no anomalous deviations are found not even near the weak regions. The rheological structure would affect more stresses in the lithosphere if the rheological weak layers were thicker, e.g., with different lithology or increment in the temperature.

The stress ratio is defined as the ratio between the equivalent stress and the yield stress. The equivalent stress is the square root of the second invariant of the stress tensor and it describes the deviatoric state of stress. The stress ratio is larger or equal to one (≥ 1) when equivalent stress exceeds the yield stress, i.e., deformation occurs and less than one (<1) when the stress state is elastic or near failure. In this model deformation corresponds to brittle or ductile mechanism depending on the affecting rheological behaviour. In Fig. 8, the stress ratio shows that with current stress, material and rheological conditions no failure exists. Areas with low rheological strength, i.e., regions in the upper and the middle crust, are the ones where deformation would first occur if prevailing conditions change, e.g., the temperature is higher. Also the surface of the model is close to failure, however, the resolution of the model restricts detailed inspection of the conditions in the first five kilometres of the model. With this modelling method the location of the earthquakes cannot be resolved in any case due to fact that we are not modelling mechanism required for earthquake to occur. In the mantle, the model depth of 100 km also limits the onset of plastic deformation. Based on the earlier 2-D models of similar type this zone of deformation would lie very near or only slightly deeper than the depth of 100 km. Fig. 9 shows

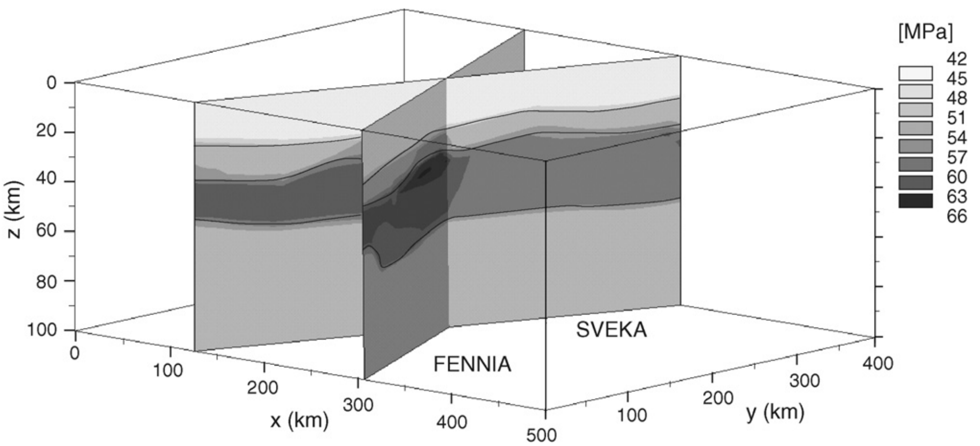

Fig. 10. Cross-sections of the stress intensity resulting from NW compression in the DSS profiles FENNIA and SVEKA.

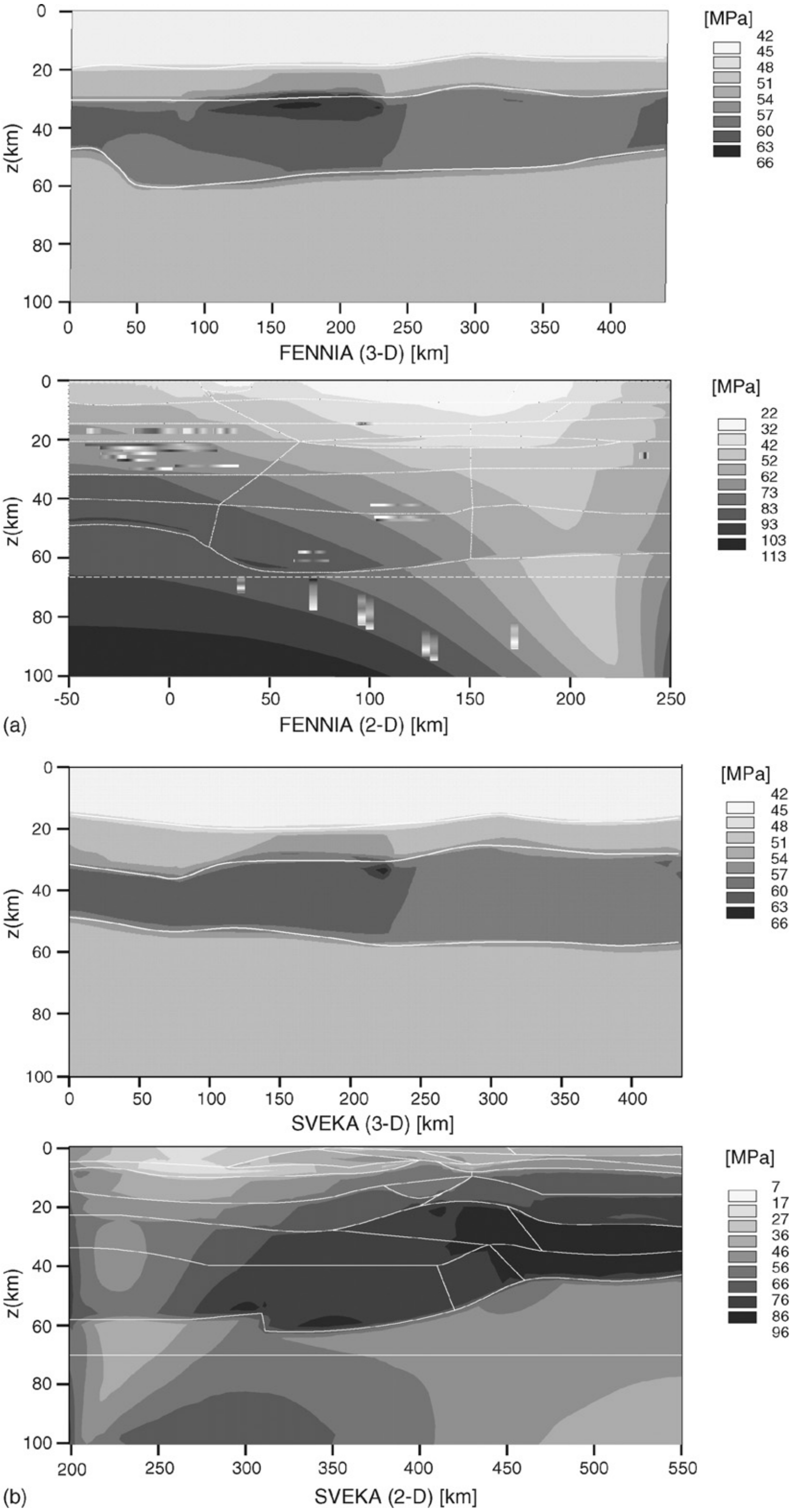

Fig. 11. (a) The stress intensity for the DSS profile FENNIA. Upper panel shows the 3-D model result as a cross-section crossing the entire model along the FENNIA profile (see Fig. 10) and lower panel the results of the 2-D model (Moisio and Kaikkonen, 2004). Horizontal coordinates are set so that 0 km is in the southern boundary of the 3-D model. Horizontal coordinates of the 2-D model are equivalent White lines show the structural boundaries. (b) The stress intensity for the DSS profile SVEKA. Upper panel shows the 3-D model result as a cross-section crossing the entire model (see Fig. 10) and lower panel the results of the 2-D model.

results as a function of depth from four different points of the model area. These locations are also shown in Fig. 1. Fig. 9a shows temperature, Fig. 9b rheological strength, Fig. 9c stress intensity and Fig. 9d focal depth histogram of earthquakes during 1965–2004 from the central Fennoscandian Shield covering the area of 18–32E and 59–65N. For the locations of these earthquakes see Fig. 3.

5.3. Comparison with 2-D models

The most significant difference in modelling between this 3-D model and with the earlier 2-D models of the SVEKA and the FENNIA profiles (Moisio and Kaikkonen, 2001, 2004) is in the direction of boundary condition. In the 2-D cases the used boundary condition is restricted to act in the direction of the seismic profile. However, this direction is not necessarily the same as the assumed direction of maximum horizontal stress. In the 3-D case the mesh itself is oriented so that the applied boundary condition is affecting in the assumed correct direction, i.e., approximately NW–SE. Differences between the 3-D and the 2-D thermal models were discussed at chapter 5.1.

The same rheological composition is used for the lithosphere in both 2- and 3-D models and major differences between them are temperature and structural boundaries of the models. Behaviour of the rheological strength is quite similar especially for the FENNIA profile, where similar weak layers in the crust are found as in the 2-D case. Also for the SVEKA profile main features are principally the same, i.e., rheologically strong layer in the lower crust. However, the weak layer found in the lower crust of the 2-D model is absent in the 3-D case. In both of the 2-D models the vertical resolution is higher, i.e., element sizes are smaller and thereby 3-D model is slightly coarser which in some amount is seen on the results. Fig. 10 shows the stress intensity for the 3-D model as cross-sections for the positions of the FENNIA and SVEKA profiles, where mainly same features are seen as in Fig. 7. In Fig. 11a and b the stress intensity is shown for the 3-D model in the upper panels (same as in Fig. 10) and for the original 2-D models in the lower panels scaled to the depth of 100 km. Note that the horizontal coordinates in these figures are equivalent. Comparison reveals that the 2-D models where the pressure boundary condition is applied, differ quite remarkably from the 3-D one with similar boundary condition. In fact, behaviour of the stress intensity is similar to the 2-D cases where the displacement boundary condition is used (not shown). Boundary effect also distorts the stresses in the 2-D cases near the relevant edge. The maximum values of the stress intensity in the 2-D models are about twice as high as in the 3-D case, although in the crust alone the magnitudes are much closer to each other. In the 3-D model, it would be possible to use larger pressure values than in the 2-D models as boundary condition as long as the resulting stress field is not in contradiction with the assumed maximum intraplate stresses. Comparison between the stress ratios (not shown) reveals that in the 2-D cases very thin weak layers where ductile deformation takes place are visible mainly due to better model resolution whereas in the 3-D model these layers are absent, In general, the resulting behaviour of the 3-D model in comparison with the 2-D cases is slightly diverse, but like the stress ratio shows no dramatic differences are found. However, the 3-D model would allow the use of anisotropic materials in any direction opening new possibilities in the future modelling.

6. Conclusions

Applied 3-D thermal, rheological and structural modelling has shown that in comparison with 2-D modelling some differences are to be expected. The calculated thermal structure of the lithosphere and especially the surface HFD becomes smoother in comparison with the measured surface HFD. The calculated surface HFD is between 40 and 48 mW m^{-2} in the Proterozoic southern part and below 40 mW m^{-2} in the older and northern Archaean part of the model. At the depth of 50 km the HFD has values between 12 and 14 mW m^{-2}. Calculated rheological structure in the 3-D model has similar features as in the earlier 2-D rheological models, although the 3-D model structure is not so fine detailed as in the 2-D cases. The rheological strength has a layered structure with two individual rheologically weak layers in the crust and strong layer in the upper part of the lower crust. The minimum BDT depth is around 10 km in the southern part of the model while in the north and north-eastern parts the BDT depth is around 45–50 km. Comparison with the focal depth data shows that most of the earthquakes are located in the brittle regime as nearly 70% of them occur no deeper than 10 km. Resulting stress conditions and possible regions of deformation after the model is subjected to pressure of 50 MPa reveals that the stress field is quite uniformly distributed in different crustal layers and that the elastic parameters control more the state of the stress than the applied rheological structure. In the upper crust the stress intensity has values between 42 and 45 MPa whereas in the middle crust the values are around 50 MPa. The highest values around 60 MPa are found in the lower crust. With such low stress levels no ductile deformation is found and areas that are close to failure can only be pointed out. Comparison with the results of the 2-D and 3-D models shows that stress distribution is totally different in these models despite the same boundary condition used. Even so the deformation in the models is quite close to each other.

Acknowledgements

We wish to thank two reviewers, I. Kukkonen and anonymous one for their useful comments and suggestions.

References

Ádám, A., Kaikkonen, P., Hjelt, S.-E., Pajunpää, K., Szarka, L., Verö, J., Wallner, A., 1982. Magnetotelluric and audiomagnetotelluric measurements in Finland. Tectonophysics 90, 77–90.

Ahjos, T., Uski, M., 1992. Earthquakes in northern Europe in 1375–1989. Tectonophysics 207, 1–123.

BABEL Working Group, 1993. Integrated seismic studies of the Baltic shield using data in the Gulf of Bothnia region. Geophys. J. Int. 112, 305–324.

Babuska, V., Plomerova, J., Padjusak, P., 1988. Seismologically determined deep lithosphere structure in Fennoscandia. Geol. Fören. Stockholm Förh. 110, 380–382.

Blanpied, M.L., Lockner, D.A., Byerlee, J.D., 1991. Fault stability inferred from granite sliding experiments at hydrothermal conditions. Geophys. Res. Lett. 18, 609–612.

Calcagnile, G., 1982. The lithosphere–astenosphere system in Fennoscandia. Tectonophysics 90, 19–35.

Carmichael, R.S., 1989. Practical Handbook of Physical Properties of Rocks and Minerals. CRC Press, Boca Raton, Florida, 714 pp.

Carter, N.L., Tsenn, M.C., 1987. Flow properties of continental lithosphere. Tectonophysics 136, 27–63.

Čermák, V., Balling, N., Kukkonen, I., Zui, V.I., 1993. Heat flow in the Baltic Shield-results of the lithospheric geothermal modelling. Precamb. Res. 64, 53–65.

Chen, R., 1991. On horizontal crustal deformation in Finland. Rep. Finn. Geod. Inst. 91 (1) 77 (Helsinki).

Cloetingh, S., Banda, E., 1992. Europe's lithosphere-physical properties. In: Blundell, D., Freeman, R., Mueller, St. (Eds.), A Continent Revealed: The European Geotraverse. Cambridge University Press, Cambridge, pp. 71–102.

Dragoni, M., Pasquale, V., Verdoya, M., Chiozzi, P., 1993. Rheological consequences of the lithospheric thermal structure in the Fennoscandian Shield. Global Plan. Change 8, 113–126.

Drury, M.R., Vissers, R.L.M., van der Wal, D., Hoogerduijn Strating, E.H., 1991. Shear localization in upper mantle peridotites. Pure Appl. Geophys. 137, 439–460.

FENNIA Working Group, 1998. P- and S-Velocity Structure of the Fennoscandian Shield Beneath the FENNIA Profile in Southern Finland, Inst. of Seismology, University of Helsinki, Report S-38, 14p.

Fernàndez, M., Ranalli, G., 1997. The role of rheology in extensional basin formation modelling. Tectonophysics 282, 129–145.

Gaal, G., Gorbatschev, R., 1987. An outline of the Precambrian evolution of Baltic Shield. Precamb. Res. 35, 15–52.

Goetze, C., Evans, B., 1979. Stress and temperature in the bending lithosphere as constrained by experimental rock mechanics. Geophys. J. R. Astr. Soc. 59, 463–478.

Grad, M., Luosto, U., 1987. Seismic models of the crust of the Baltic shield along the SVEKA profile in Finland. Ann. Geophys. 5B, 639–650.

Jokinen, J., Kukkonen, I., 1999. Random modelling of the lithospheric thermal regime: forward simulations applied in uncertainty analysis. Tectonophysics 306, 277–292.

Jokinen, J., Kukkonen, I.T., 2000. Inverse Monte Carlo simulation of the lithospheric thermal regime in the Fennoscandian Shield using xenolith-derived mantle temperatures. J. Geodyn. 29, 71–85.

Järvimäki, P., Puranen, M., 1979. Heat flow measurements in Finland. In: Cermak, V., Rybach, L. (Eds.), Terrestial Heat Flow in Europe. Springer, Berlin, pp. 172–178.

Jõeleht, A., Kukkonen, I.T., 1998. Thermal properties of granulite facies rocks in the Precambrian basement of Estonia and Finland. Tectonophysics 291, 195–203.

Kaikkonen, P., Vanyan, L.L., Hjelt, S.-E., Shilovsky, A.P., Pajunpää, K., Shilovsky, P.P., 1983. A preliminary geoelectrical model of the Karelian megablock of the Baltic Shield. Phys. Earth Planet. Inter. 32, 301–305.

Kaikkonen, P., Moisio, K., Heeremans, M., 2000. Thermomechanical lithospheric structure of the central Fennoscandian Shield. Phys. Earth Planet. Inter. 119, 209–235.

Kakkuri, J., 1997. Postglacial deformation of the Fennoscandian crust. In: Pesonen, L.J. (Ed.), The Lithosphere in Finland – A Geophysical Perspective. Geophysica, vol. 33, pp. 99–109.

Klasson, H., Lejon, B., 1990. Rock Stress Measurements in the Deep Boreholes at Kuhmo, Hyrynsalmi, Sievi, Eurajoki and Konginkangas. Technical report YJT-90-18. Nuclear Waste Commission of Finnish Power Companies, 122 pp.

Korja, T., 1997. Electrical conductivity of the lithosphere-implications for the evolution of the Fennoscandian Shield. In: Pesonen, L.J. (Ed.), The Lithosphere in Finland – A Geophysical Perspective. Geophysica, vol. 33, pp. 17–50.

Korja, T., Hjelt, S.-E., 1993. Electromagnetic studies in the Fennoscandian Shield-electrical conductivity of Precambrian crust. Phys. Earth Planet. Inter. 81, 107–138.

Korja, A., Heikkinen, P.J., 1995. Proterozoic extensional tectonics of the central Fennoscandian Shield: results from the BABEL experiment. Tectonics 14, 504–517.

Kukkonen, I.T., 1988. Terrestrial heat flow and groundwater circulation in the bedrock in the central Baltic Shield. Tectonophysics 156, 59–74.

Kukkonen, I.T., 1989a. Terrestrial heat flow in Finland, the central Fennoscandian Shield. Geological Survey of Finland, Nuclear Waste Disposal Research. Report YST-68, 99 pp.

Kukkonen, I.T., 1989b. Terrestrial heat flow and radiogenic heat production in Finland, the central Baltic Shield. In: Cermák, V., Rybach, L., Decker, E.R. (Eds.), Heat Flow and Lithosphere Structure. Tectonophysics, vol. 164, pp. 219–230.

Kukkonen, I.T., 1993. Heat flow map of northern and central parts of the Fennoscandian Shield based on geochemical surveys of heat producing elements. Tectonophysics 225, 3–13.

Kukkonen, I.T., 1995. Thermal aspects of groundwater circulation in bedrock and its effect on crustal geothermal modelling in Finland, the central Fennoscandian Shield. Tectonophysics 244, 119–136.

Kukkonen, I.T., 1998. Temperature and heat flow density in a thick cratonic lithosphere: the SVEKA transect, central Fennoscandian Shield. J. Geodyn. 26, 111–136.

Kukkonen, I.T., Jõeleht, A., 1996. Geothermal modelling of the lithosphere in the central Baltic Shield and its southern slope. Tectonophysics 255, 25–45.

Kukkonen, I.T., Peltonen, P., 1999. Xenolith-controlled geotherm for the central Fennoscandian Shield: implications for lithophere–asthenosphere relations. Tectonophysics 304, 301–315.

Kukkonen, I.T., Lahtinen, R., 2001. Variation of radiogenic heat production rate in 2.8–1.8 Ga old rocks in the central Fennoscandian Shield. Phys. Earth Planet. Inter. 12, 279–294.

Kukkonen, I.T., Jõeleht, A., 2003. Weichselian temperatures from geothermal heat flow data. J. Geophys. Res. 108, B3.

Kukkonen, I.T., Jokinen, J., Seipold, U., 1999. Temperature and pressure dependencies of thermal transport properties of rocks: implications for uncertainties in thermal lithosphere models and new laboratory measurements of high-grade rocks in the central Fennoscandian Shield. Surv. Geophys. 20, 33–59.

Kukkonen, I., Heikkinen, P., Ekdahl, E., Korja, A., Hjelt, S.-E., Yliniemi, J., Berzin, R., FIRE Working Group, 2002. Project FIRE: Deep Seismic Reflection Sounding in Finland 2001–2005, Julkaisussa; Lahtinen, R., Korja, A., Arhe, K., Eklund, O., Hjelt, S.-E., Pesonen, L.J. (Eds.), 2002. Lithosphere 2002 – Second Symposium on the Structure, Composition and Evolution of the Lithosphere in Finland. Programme and Extended Abstracts, Espoo, Finland, November 12–13, Institute Seismology, University of Helsinki, Report S-42, pp. 67–70.

Kukkonen, I.T., Kinnunen, K.A., Peltonen, P., 2003. Mantle xenoliths and thick lithosphere in the Fennoscandian Shield. Phys. Chem. Earth 28, 349–360.

Kozlovskaya, E., Yliniemi, J., 1999. Deep structure of the earth's crust along the SVEKA profile and its extention to the north-east. Geophysica 35, 111–123.

Lamontagne, M., Ranalli, G., 1996. Thermal and rheological constraints on the earthquake depth distribution in the Charlevoix, Canada, intraplate seismic zone. Tectonophysics 257, 55–69.

Lehtinen, M., Nurmi, P.A., Rämö, O.T. (Eds.), 2005. Precambrian Geology of Finland. Key to the Evolution of the Fennoscandian Shield. Elsevier, 750 pp.

Luosto, U., 1997. Structure of the earth's crust in Fennoscandia as revealed from refraction and wide-angle reflection studies. In: Pesonen, L.J. (Ed.), The Lithosphere in Finland – a Geophysical Perspective. Geophysica, vol. 33, pp. 3–16.

Luosto, U., Tiira, T., Korhonen, H., Azbel, I., Burmin, V., Buyanov, A., Kosminskaya, I., Ionkis, V., Sharov, N., 1990. Crust and upper mantle structure along the DSS BALTIC profile in SE Finland. Geophys. J. Int. 101, 89–110.

Luosto, U., Grad, M., Guterch, A., Heikkinen, P., Janik, T., Komminaho, K., Lund, C., Thybo, H., Yliniemi, J., 1994. Crustal structure along the SVEKA'91 profile in Finland. In: Makropoulos, K., Suhadolc, P. (Eds.), European Seismological Commission, XXIV General Assembly, 1994. September 19–24, Athens, Greece. Proceedings and Activity Report 1992–1994, vol. II, pp. 974–983.

Moisio, K., Kaikkonen, P., Beekman, F., 2000. Rheological structure and dynamical response of the DSS profile BALTIC in the SE Fennoscandian Shield. Tectonophysics 320, 175–194.

Moisio, K., Kaikkonen, P., 2001. Geodynamics and rheology along the DSS profile SVEKA'81 in the central Fennoscandian Shield. Tectonophysics 340, 61–77.

Moisio, K., Kaikkonen, P., 2004. The present day rheology, stress field and deformation along the DSS profile FENNIA in the central Fennoscandian Shield. J. Geodyn. 38, 161–184.

Ord, A., Hobbs, B., 1989. The strength of the continental crust detachments zones and the development of plastic instabilities. Tectonophysics 158, 269–289.

Pasquale, V., Verdoya, M., Chiozzi, P., 1991. Lithospheric thermal structure in the Baltic shield. Geophys. J. Int. 106, 611–620.

Pasquale, V., Verdoya, M., Chiozzi, P., 2001. Heat flux and the seismicity in the Fennoscandian Shield. Phys. Earth Planet. Inter. 126, 147–162.

Puranen, M., Järvimäki, P., Hämäläinen, U., Lehtinen, S., 1968. Terrestial heat flow in Finland. Geoexploration 6, 151–162.

Ranalli, G., 1995. Rheology of the Earth, second ed. Chapman & Hall, London, 413 pp.

Ranalli, G., 2000. Rheology of the crust and its role in tectonic reactivation. J. Geodyn. 30, 3–15.

Reinecker, J., Heidbach, O., Tingay, M., Connolly, P., Müller, B., 2004. The 2004 Release of the World Stress Map. (Available online at www.world-stress-map.org).

Saari, J., 1992. A Review of the Seismotectonics of Finland. Nuclear Waste Commission of Finnish Power Companies, Report YJT-92-99, 76 pp.

Sandoval, S., Kissling, E., Ansorge, J., The SVEKALAPKO Seismic Tomography Working Group, 2004. High-resolution body wave tomography beneath the SVEKALAPKO array—II. Anomalous upper mantle structure beneath the central Baltic Shield. Geophys. J. Int. 157, 200–214.

Shimada, M., 1993. Lithosphere strength inferred from fracture strength of rocks at high confining pressures and temperatures. Tectonophysics 217, 55–64.

Scholz, C.H., 1990. The Mechanics of Earthquakes and Faulting. Cambridge University Press, Cambridge, 439 pp.

Tsenn, M.C., Carter, N.L., 1987. Upper limits of power law creep of rocks. Tectonophysics 136, 1–26.

Uski, M., Hyvönen, T., Korja, A., Airo, M.-L., 2003. Focal mechanisms of three earthquakes in Finland and their relation to surface faults. Tectonophysics 363, 141–157.

Uski, M., Pelkonen, E., 2004. Earthquakes in Northern Europe in 2003. Inst. Seismology, Univ. Helsinki, Report R-206. (Available online at: www.seismo.helsinki.fi).

Wilks, J.C., Carter, N.L., 1990. Rheology of some continental lower crustal rocks. Tectonophysics 182, 57–77.

Yliniemi, J., Jokinen, J., Luukkonen, E., 1996. Deep structure of the Earth's crust along the GGT/SVEKA transect extension to northeast. In: Ekdahl, E., Autio, S., (Eds.), Global Geoscience Transect/SVEKA – Proceedings of the Kuopio Seminar, Finland 25.–26.11.1993. Geological Survey of Finland, Report of Investigation 136, p. 56.